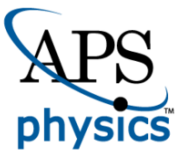

Spin-Triplet Pairing State Evidenced by Half-Quantum Flux in a Noncentrosymmetric Superconductor

Xiaoying Xu, Yufan Li, and C. L. Chien

Phys. Rev. Lett. **124**, 167001 — Published 22 April 2020

DOI: 10.1103/PhysRevLett.124.167001

Spin-triplet pairing state evidenced by half-quantum flux in a noncentrosymmetric superconductor

Xiaoying Xu, Yufan Li, and C. L. Chien

Department of Physics and Astronomy,

The Johns Hopkins University, Baltimore, MD 21218, USA

(Dated: March 13, 2020)

Abstract

A prime category of superconducting materials in which to look for spin-triplet pairing and topological superconductivity are superconductors without inversion symmetry. It is predicted that the broken parity symmetry gives rise to an admixture of spin-triplet and spin-singlet pairing states. However, experimental confirmation of pairing mixing in any material remains elusive. In this work, we perform phase-sensitive experiment to examine the pairing state of noncentrosymmetric superconductor α–BiPd. The Little-Parks effect observed in mesoscopic polycrystalline α–BiPd rings reveals the presence of half-integer magnetic flux quantization, which provides a decisive evidence for the spin-triplet pairing state. We find both half-quantum fluxes and integer-quantum fluxes of different proportions, consistent with the scenario of an admixture of singlet-triplet pairing.

The superconducting Cooper pair is a system of two spin-$\frac{1}{2}$ particles with total spin angular momentum of either 0 as a spin-singlet state, or 1 as a spin-triplet state. The spin-singlet pairing is found to be the case for the overwhelming majority of known superconductors (SCs), including s-wave SCs and d-wave high-T_c cuprates. In contrast, far fewer superconducting materials exhibit spin-triplet pairing. The search for spin-triplet SCs intensifies in recent years with the surging interest in topological superconductors [1]. It is shown that with few exceptions, spin-triplet SCs are inherently topological [2–5] and therefore ideal for realizing Majorana fermions [6, 7].

For SCs with inversion symmetry, the parity symmetry imposes constraint on the pairing state, which must be either spin-singlet with even-parity or spin-triplet with odd-parity [8]. For noncentrosymmetric SCs, on the other hand, the broken parity symmetry compels an admixture of singlet and triplet pairing states but with unspecified fractions [9–12]. Although superconducting materials without inversion symmetry are not rare, many appear to be s-wave SCs [12, 13]. Monoclinic α–BiPd is one noncentrosymmetric (space group $P2_1$) superconductor [14, 15]. However, experimental results from scanning tunneling spectroscopy [16], upper critical field and heat capacity measurements [17, 18] indicate that the superconducting state is predominately singlet s-wave with a nodeless single gap. This has led to the view that the parity-breaking spin-orbit coupling induced by noncentrosymmetry may be too weak to realize any observable effect [5, 13, 18]. However, this is at odds with the findings of multiple superconducting gaps as observed by point-contact Andreev reflection [19] and penetration depth measurement [20], which support singlet-triplet admixture. Other studies also report unusual properties such as the suppression of the coherence peak of the spin-lattice relaxation rate in NMR measurement [21], weak ferromagnetism near the transition temperature [22], and topological band structure inferred from quantum oscillations [23]. Furthermore, the presence of topological Dirac surface states have been reported by several photoemission studies [24–26]. It should be noted that these experiments were conducted above the superconducting transition temperature, and that there are discrepancies in the interpretations of the observed band structure [27].

These suggestive and conflicting results notwithstanding, it is essential to perform not amplitude-sensitive, but phase-sensitive measurements of the pairing state of α–BiPd [28]. The single-value nature of the complex superconducting wave function demands a universal phase change of 2π in any closed path around a ring, which leads to magnetic flux quantiza-

tion [29]. As it was first and repeatedly demonstrated in s-wave SCs, the fluxoid quantizes in integer numbers of flux quanta, or $\Phi' = n\Phi_0$, where $\Phi_0 = hc/2e$ [30]. On the other hand, the anisotropic spin-triplet pairing state may induce an additional π phase shift at crystalline grain boundaries [31], leading to half-quantum flux (HQF) of $\Phi' = (n+1/2)\Phi_0$. As we have demonstrated in the case of centrosymmetric β–Bi_2Pd, the anisotropic gap function of the spin-triplet pairing symmetry can be unambiguously evidenced by HQF quantization in polycrystalline rings [32]. The distinctive experimental signature of HQF can be particularly powerful in determining the spin-triplet component in the presumed singlet-triplet admixture. In this work, we perform Little-Parks experiment [33] to determine the magnetic flux quantization in polycrystalline rings of noncentrosymmetric α–BiPd. We report the observation of HQFs as well as integer-flux quantization, providing a conclusive evidence for the presence of admixture of singlet-triplet pairing in a noncentrosymmetric SC.

We used magnetron sputtering to deposite 50 nm-thick α–BiPd thin films onto $SrTiO_3$ (001) substrates held at elevated temperature of 400 ^{o}C, which were capped with 1 nm-thick MgO protecting layer before removing from the vacuum chamber. X-ray diffrection shows the α–BiPd films are $(1\overline{1}2)$-textured [Fig. 1(c)], whereas the pole-figure measurements show these films are polycrystalline textured without in-plane epitaxy [34]. The α–BiPd films become superconducting at the T_c of 3.6 K with a sharp transition of less than 0.1 K, similar to those of bulk specimens [17].

The Little-Parks effect concerns the periodic oscillation of the free energy, and the resultant oscillation of T_c, as a function of the applied magnetic flux threading through a superconducting ring [33]. Experimentally, one measures the electric resistance R of the patterned ring at a fixed temperature slightly below T_c. The experimental setup is depicted in Fig. 1(b), where the external magnetic field is applied perpendicular to the plane of the ring device, or along z direction. The Little-Parks effect for the well-known integer-flux quantization of $\Phi' = n\Phi_0$ is schematically presented in Fig. 1(d), where the resistance minima occur when the applied magnetic flux equals integer number of Φ_0, including the zero field. In the unusual case of HQF, the anisotropic gap function induces a π phase shift resulting with the quantization condition of $\Phi' = (n + 1/2)\Phi_0$ [31] as shown in Fig. 1(e), where the resistance minima occur at half-integer number of Φ_0 . This HQF scenario can be realized by the anisotropic gap function of spin-triplet pairing [31].

To examine the Little-Parks effect, we patterned the α–BiPd thin films into various sub-

μm-sized ring devices by electron beam lithography. The dimensions of the rings are chosen so that the oscillation period in term of magnetic field is reasonably large (> 20 Oe), and that the zero-external-field state can be unequivocally determined [32]. A scanning electron microscopy (SEM) image of a representative α–BiPd ring device is shown in Fig. 1(b). Common to the sub-micron-sized devices, the superconducting transition broadens [34].

The Little-Parks effect distinctively reveals the presence of HQFs in polycrystalline α–BiPd rings. In Fig. 2 we show one such example, in device A, a 450 nm × 450 nm square ring. The observed oscillation period of 106.2 Oe is in good agreement with the expected value of 102.1 Oe calculated from the enclosed area of the ring [34]. As shown in the upper panel of Fig. 2(a), the oscillations are superimposed on top of a roughly parabolic-shaped background, commonly observed in Little-Parks experiments [33, 35, 36]. One may subtract the background, which can be well described by a polynominal function of field (black dashed line) [34] and obtain the oscillatory component ΔR versus H as shown in the lower panel of Fig. 2(a). The resistance reaches minima at the half-integer numbers of Φ_0, the scenario of HQF as depicted in Fig. 1(e).

We performed extensive experiments to ascertain HQF, particularly to exclude the artifact of possible trapped magnetic flux [32]. The Little-Parks oscillation shown in Fig. 2(a) is symmetric with respect to the zero magnetic field, indicating that the π phase shift is not due to defect-trapped vortices. We also did measurements by sweeping the magnetic field in two opposite directions, as shown in Fig. 2(b). Before each scan, the sample was first warmed up to 10 K, then cooled down in zero magnetic field. The opposite field scans yield virtually identical results, with no indication of trapped flux. The Little-Parks effect is observed in an extended temperature range, as shown in Fig. 2(b), where the HQF remains robust at various temperatures.

In addition to device A, we have also observed HQFs in two other rings, in devices B and C, with results shown in Fig. 3. The π phase shift with HQF can be observed at various temperatures and in both field sweeping directions. The three rings that show HQF have different geometric factors: device A (450 nm × 450 nm), devices B (500 nm × 500 nm) and device C (800 nm × 800 nm) have different line widths of 50 nm, 100 nm and 100 nm, respectively. The observation of HQFs is a decisive evidence for the presence of a spin-triplet pairing component in α–BiPd.

The gap function of spin-triplet pairing has odd-parity, i.e., $\Delta_k = -\Delta_{-k}$. A sign change

can occur at certain crystalline grain boundaries, inducing a π phase shift which gives rise to HQF [31]. The realization of HQF is contingent upon the total number of such crystalline grain boundaries that produce such π phase shift, or π-junctions [28, 31, 32]. Over the circumference of the ring, only an odd number of π-junctions would produce a net phase change of π, which leads to a HQF-hosting π-ring. For an even number of π-junctions where the total phase changes add up to 2π, the loop would show integer flux quantization, or a 0-ring. This is indeed the case of noncentrosymmetric α–BiPd. In addition to π-rings, we have also observed 0-rings, as shown in Fig. 4, in devices A1, B1 and C1, which share the same design geometries with the three π-ring counterparts of devices A, B and C, respectively. They manifest integer-quantum flux quantization of $\Phi' = n\Phi_0$, as depicted in Fig. 1(d). The presence of π-rings and 0-rings conclusively show the noncentrosymmetric α–BiPd has spin-triplet pairing.

For a pure spin-triplet pairing state, it is equally probable for a polycrystalline ring to be either a π-ring or a 0-ring. This is indeed the case for the centrosymmetric β–Bi_2Pd, where our experiments found about 60% of the total 21 polycrystalline rings are π-rings, whilst the rest are 0-rings [32]. On the other hand, no π-rings shall be expected in ring devices of *epitaxial* β–Bi_2Pd, due to the lack of any π-junctions with the absence of grain boundaries; and none was observed [32, 37]. For a pure spin-singlet *s*-wave SC, the isotropic pairing state cannot form any π-junctions at all, with or without grain boundaries. There can be only 0-rings with no π-rings, regardless of the crystalline nature of the sample.

For noncentrosymmetric SCs, the pairing state is expected to be an admixture of singlet and triplet. The proportion of π-ring can vary between the two extremes of pure singlet (0% of all devices) and pure triplet (close to 50% of all devices), assuming that in the polycrystalline specimen the crystalline orientations of the grains are random. For a total of 16 α–BiPd rings, we have observed 3 π-rings and 13 0-rings, i.e., less than 20% polycrystalline α–BiPd devices are π-rings. The intermediate π-ring proportion suggests an admixture of singlet and triplet pairing states in noncentrosymmetric α–BiPd.

In summary, we have examined the flux quantization in α–BiPd, a noncentrosymmetric superconductor where singlet-triplet pairing mixing is expected. We have observed HQF, a decisive evidence for the presence of a spin-triplet pairing component. With the confirmation of spin-triplet pairing, α–BiPd is a strong candidate for topological SC. The ultimate challenge would be to observe the Majorana states in this material.

An emerging paradigm is to identify anisotropic pairing states by observing HQF in polycrystalline ring devices, as we have demonstrated in β–Bi_2Pd [32] earlier and α–BiPd in this work. The experimental signature of HQF is unambiguous for distinguishing the triplet pairing component. It would be particularly interesting to apply this phase-sensitive technique to other noncentrosymmetric SCs, where a mixed pairing state is generally expected.

We gratefully acknowledge the support from the U.S. Department of Energy (DOE), Basic Energy Science award no. DESC0009390. Xiaoying Xu was supported in part by SHINES, an EFRC funded by U.S. DOE Basic Energy Science award no. SC0012670.

[1] X.-L. Qi and S.-C. Zhang, Reviews of Modern Physics **83**, 1057 (2011), URL https://link.aps.org/doi/10.1103/RevModPhys.83.1057.

[2] L. Fu and E. Berg, Physical Review Letters **105**, 097001 (2010), URL https://link.aps.org/doi/10.1103/PhysRevLett.105.097001.

[3] M. Sato, Physical Review B **81**, 220504(R) (2010), URL https://link.aps.org/doi/10.1103/PhysRevB.81.220504.

[4] X.-L. Qi, T. L. Hughes, and S.-C. Zhang, Physical Review B **81**, 134508 (2010), URL https://link.aps.org/doi/10.1103/PhysRevB.81.134508.

[5] M. Sato and Y. Ando, Reports on Progress in Physics **80**, 076501 (2017), ISSN 0034-4885, URL http://stacks.iop.org/0034-4885/80/i=7/a=076501.

[6] N. Read and D. Green, Physical Review B **61**, 10267 (2000), URL https://link.aps.org/doi/10.1103/PhysRevB.61.10267.

[7] A. Y. Kitaev, Physics-Uspekhi **44**, 131 (2001), ISSN 1063-7869, URL http://stacks.iop.org/1063-7869/44/i=10S/a=S29.

[8] P. W. Anderson, Physical Review B **30**, 4000 (1984), URL https://link.aps.org/doi/10.1103/PhysRevB.30.4000.

[9] L. P. Gor'kov and E. I. Rashba, Physical Review Letters **87**, 037004 (2001), URL https://link.aps.org/doi/10.1103/PhysRevLett.87.037004.

[10] P. A. Frigeri, D. F. Agterberg, A. Koga, and M. Sigrist, Physical Review Letters **92**, 097001 (2004), URL https://link.aps.org/doi/10.1103/PhysRevLett.92.097001.

[11] S. Fujimoto, Journal of the Physical Society of Japan **76**, 051008 (2007), URL https://doi.

org/10.1143/JPSJ.76.051008.

[12] S. Yip, Annual Review of Condensed Matter Physics **5**, 15 (2014), URL https://doi.org/10.1146/annurev-conmatphys-031113-133912.

[13] E. Bauer and M. Sigrist, eds., *Non-Centrosymmetric Superconductors* (Springer Berlin Heidelberg, 2012).

[14] N. E. Alekseevskii, Zhurnal Eksperimentalnoi I Teoreticheskoi Fiziki **23**, 484 (1952).

[15] Y. Bhatt and K. Schubert, Journal of the Less Common Metals **64**, P17 (1979) URL https://doi.org/10.1016/0022-5088(79)90184-X.

[16] Z. Sun, M. Enayat, A. Maldonado, C. Lithgow, E. Yelland, D. C. Peets, A. Yaresko, A. P. Schnyder, and P. Wahl, Nature Communications **6**, 6633 (2015), ISSN 2041-1723, URL http://www.nature.com/articles/ncomms7633.

[17] B. Joshi, A. Thamizhavel, and S. Ramakrishnan, Physical Review B **84**, 064518 (2011), URL https://link.aps.org/doi/10.1103/PhysRevB.84.064518.

[18] D. C. Peets, A. Maldonado, M. Enayat, Z. Sun, P. Wahl, and A. P. Schnyder, Physical Review B **93**, 174504 (2016), URL https://link.aps.org/doi/10.1103/PhysRevB.93.174504.

[19] M. Mondal, B. Joshi, S. Kumar, A. Kamlapure, S. C. Ganguli, A. Thamizhavel, S. S. Mandal, S. Ramakrishnan, and P. Raychaudhuri, Physical Review B **86**, 094520 (2012), URL https://link.aps.org/doi/10.1103/PhysRevB.86.094520.

[20] L. Jiao, J. L. Zhang, Y. Chen, Z. F. Weng, Y. M. Shao, J. Y. Feng, X. Lu, B. Joshi, A. Thamizhavel, S. Ramakrishnan, H.Q. Yuan, Physical Review B **89**, 060507(R) (2014), URL https://link.aps.org/doi/10.1103/PhysRevB.89.060507.

[21] K. Matano, S. Maeda, H. Sawaoka, Y. Muro, T. Takabatake, B. Joshi, S. Ramakrishnan, K. Kawashima, J. Akimitsu, and G.-q. Zheng, Journal of the Physical Society of Japan **82**, 084711 (2013), ISSN 0031-9015, URL https://journals.jps.jp/doi/10.7566/JPSJ.82.084711.

[22] R. Jha, R. Goyal, P. Neha, V. K. Maurya, A. K. Srivastava, A. Gupta, S. Patnaik, and V. P. S. Awana, Superconductor Science and Technology **29**, 025008 (2015), ISSN 0953-2048, URL https://doi.org/10.1088/0953-2048/29/2/025008.

[23] M. A. Khan, D. E. Graf, I. Vekhter, D. A. Browne, J. F. DiTusa, W. A. Phelan, and D. P. Young, Physical Review B **99**, 020507(R) (2019), URL https://link.aps.org/doi/10.1103/PhysRevB.99.020507.

[24] S. Thirupathaiah, S. Ghosh, R. Jha, E. D. L. Rienks, K. Dolui, V. V. Ravi Kishore, B. Büchner, T. Das, V. P. S. Awana, D. D. Sarma, et al., Physical Review Letters **117**, 177001 (2016), URL https://link.aps.org/doi/10.1103/PhysRevLett.117.177001.

[25] M. Neupane, N. Alidoust, M. M. Hosen, J.-X. Zhu, K. Dimitri, S.-Y. Xu, N. Dhakal, R. Sankar, I. Belopolski, D. S. Sanchez, et al., Nature Communications **7**, 13315 (2016), ISSN 2041-1723, URL https://doi.org/10.1038/ncomms13315.

[26] H. M. Benia, E. Rampi, C. Trainer, C. M. Yim, A. Maldonado, D. C. Peets, A. Stöhr, U. Starke, K. Kern, A. Yaresko, G. Levy, A. Damascelli, C.R . Ast, A. P. Schnyder, P. Wahl, et al., Physical Review B **94**, 121407(R) (2016), URL https://link.aps.org/doi/10.1103/PhysRevB.94.121407.

[27] A. Yaresko, A. P. Schnyder, H. M. Benia, C.-M. Yim, G. Levy, A. Damascelli, C. R. Ast, D. C. Peets, and P. Wahl, Physical Review B **97**, 075108 (2018), URL https://link.aps.org/doi/10.1103/PhysRevB.97.075108.

[28] C. C. Tsuei and J. R. Kirtley, Reviews of Modern Physics **72**, 969 (2000), URL https://link.aps.org/doi/10.1103/RevModPhys.72.969.

[29] N. Byers and C. N. Yang, Physical Review Letters **7**, 46 (1961), URL https://link.aps.org/doi/10.1103/PhysRevLett.7.46.

[30] B. S. Deaver and W. M. Fairbank, Physical Review Letters **7**, 43 (1961), URL https://link.aps.org/doi/10.1103/PhysRevLett.7.43.

[31] V. B. Geshkenbein, A. I. Larkin, and A. Barone, Physical Review B **36**, 235 (1987), ISSN 0163-1829, URL https://link.aps.org/doi/10.1103/PhysRevB.36.235.

[32] Y. Li, X. Xu, M.-H. Lee, M.-W. Chu, and C. L. Chien, Science **366**, 238 (2019), ISSN 0036-8075, https://science.sciencemag.org/content/366/6462/238.full.pdf, URL https://science.sciencemag.org/content/366/6462/238.

[33] W. A. Little and R. D. Parks, Physical Review Letters **9**, 9 (1962), URL https://link.aps.org/doi/10.1103/PhysRevLett.9.9.

[34] See Supplementary Material at URL for details of pole-figure measurements, critical temperature, Φ_0 calculation and raw data with the background fitting.

[35] M. Tinkham, Physical Review **129**, 2413 (1963), URL https://link.aps.org/doi/10.1103/PhysRev.129.2413.

[36] V. V. Moshchalkov, L. Gielen, C. Strunk, R. Jonckheere, X. Qiu, C. V. Haesendonck, and

Y. Bruynseraede, Nature **373**, 319 (1995), ISSN 1476-4687, URL https://doi.org/10.1038/373319a0.

[37] Y. Li, X. Xu, S.-P. Lee, and C. L. Chien, arXiv 2003.00603, URL https://arxiv.org/abs/2003.00603.

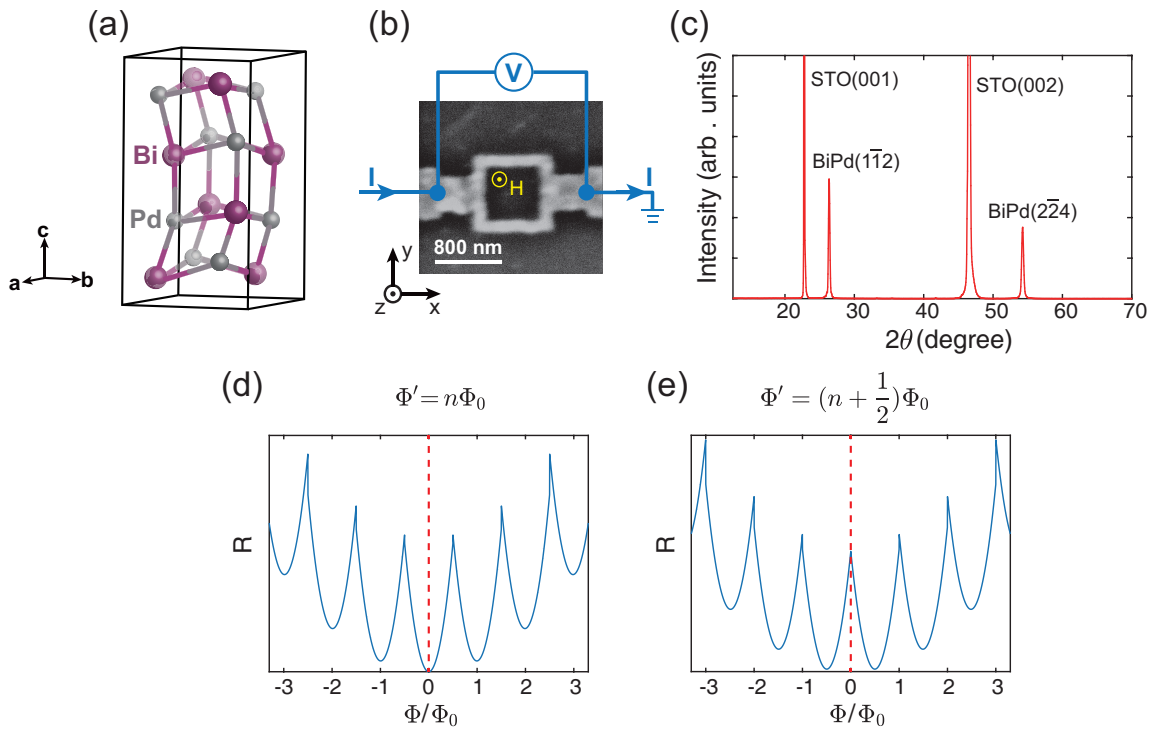

FIG. 1. (a) Crystal structure of noncentrosymmetric superconductor α-BiPd with space group $P2_1$. The lattice parameters are: a = 5.635Å, b = 5.661Å, c = 10.651Å, and γ = 100.85°. (b) The experimental setup of the ring structure with an out-of-plane magnetic field while the resistance is measured with a d.c. bias current of 1 µA. The distance between the two opposing walls is 800 nm and the width of the side wall is 100 nm (device C). The magnetic field is applied along $+z$ direction, normal to the film surface. (c) X-ray diffraction spectrum of 50 nm-thick α–BiPd thin film grown on $SrTiO_3$(001) substrate, which shows the (1$\bar{1}$2)-textured plane of α–BiPd parallel to the (001) plane of $SrTiO_3$. Schematic drawing of the Little-Parks effect of a 0-ring (d) with integer flux quantization: $\Phi' = n\Phi_0$ and a π-ring (e) with half-integer flux quantization: $\Phi' = (n + 1/2)\Phi_0$.

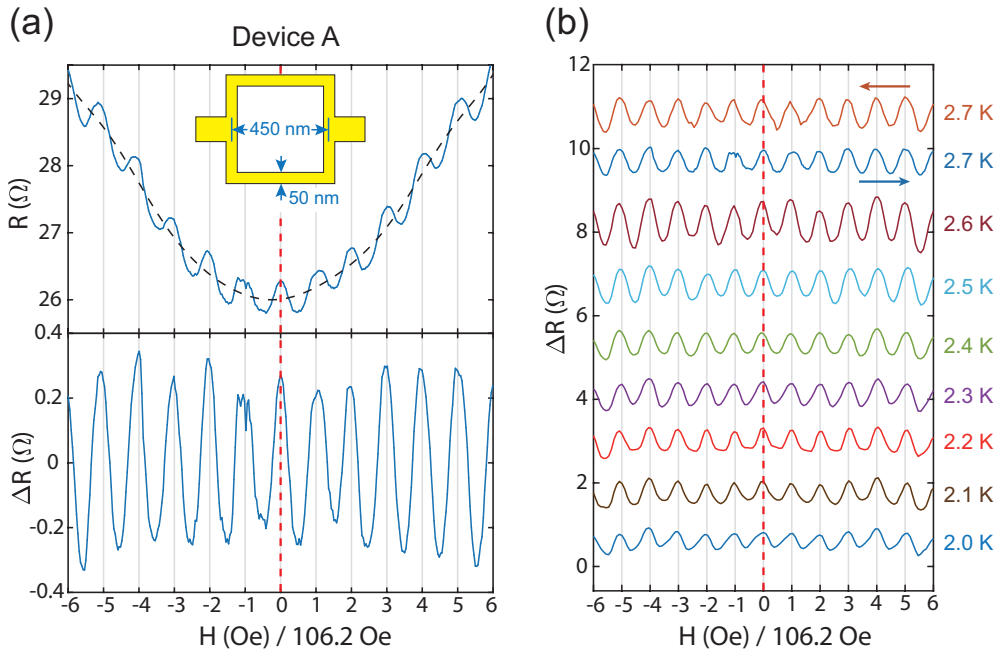

FIG. 2. Little-Parks effect of device A. (a) Upper panel: resistance as a function of applied magnetic field at 2.7 K. The red vertical dashed line denotes the zero field and the grey lines denote the fields at $n\Phi_0$. Device A has an enclosed area of 450 nm by 450 nm, which leads to an expected oscillation period of 102.1 Oe. The black dashed line is the fitted background curve. Lower panel: Little-Parks oscillation after subtraction of the background. (b) Temperature dependence of Little-Parks oscillations from 2 K to 2.7 K. The two curves at 2.7 K are obtained when sweeping the magnetic field in opposite directions.

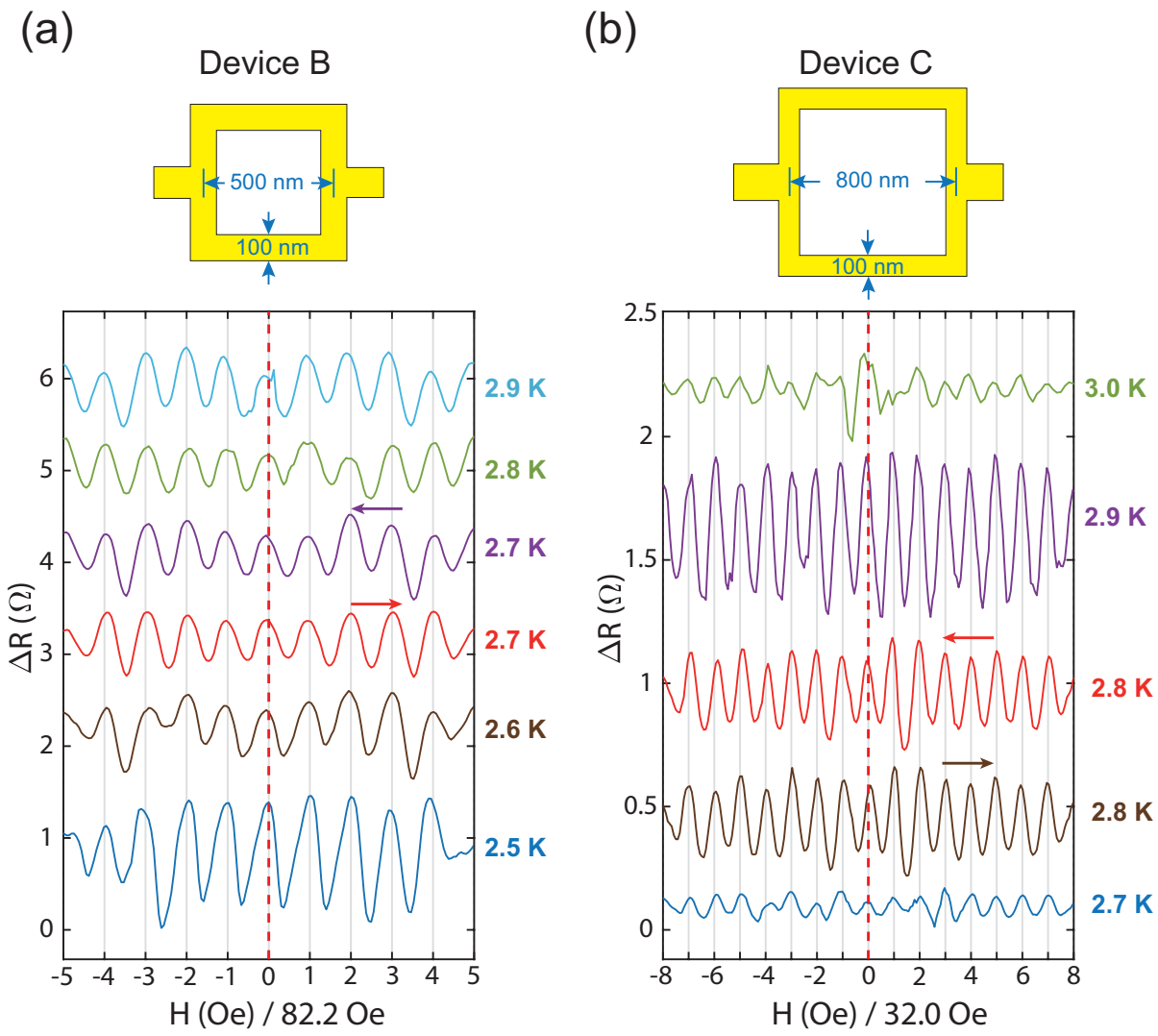

FIG. 3. Little-Parks effect at various temperatures of (a) Device B with the ring geometry of 500 nm × 500 nm, and (b) Device C with the ring geometry of 800 nm × 800 nm. The expected Φ_0-period calculated from the design geometry is 82.7 Oe for device B and 32.3 Oe for device C, respectively.

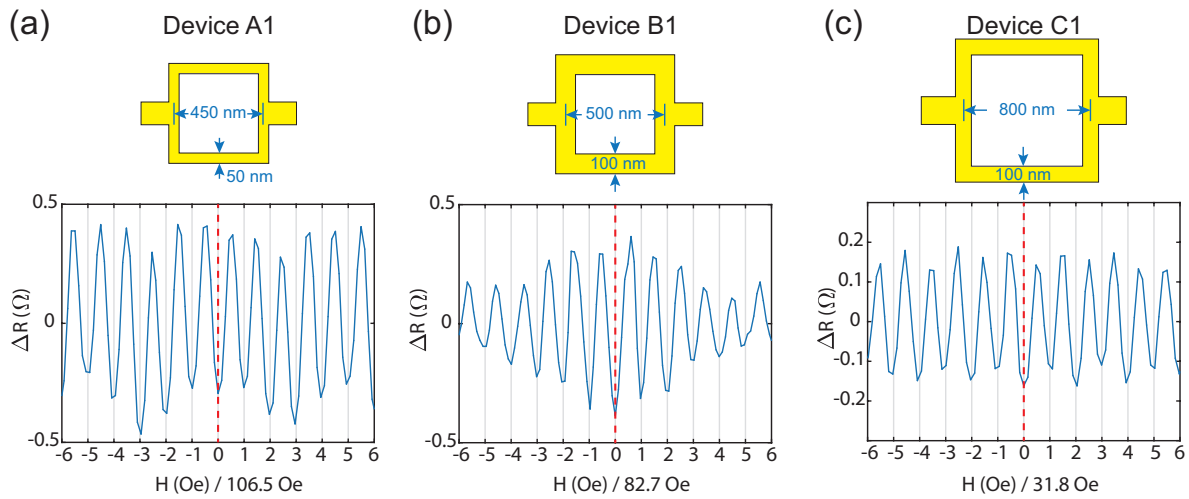

FIG. 4. Little-Parks effect of three 0–ring devices. (a) Device A1 (450 nm × 450 nm) at 2.6 K. (b) Device B1 (500 nm × 500 nm) at 2.9 K. (c) Device C1 (800 nm × 800 nm) at 2.9 K. The expected Φ_0-period calculated from the design geometry is 102.1 Oe for device A1, 82.7 Oe for device B1, and 32.3 Oe for device C1.